

## Calculation of the field-emission current from a surface using the Bardeen transfer Hamiltonian method

R. Ramprasad, L. R. C. Fonseca, and Paul von Allmen

*Motorola Inc., Flat Panel Display Division, 7700 South River Parkway, FPD22, Tempe, Arizona 85284*

(Received 1 October 1999; revised manuscript received 23 February 2000)

We have developed a method for calculating the field-emission current from a clean or adsorbate-covered metal surface using the transfer Hamiltonian method of Bardeen. The present formalism can be incorporated in accurate atomistic electronic structure methods, and so is capable of addressing system specific band structure effects, adsorbate-induced resonances, and is amenable to accurate treatments of the exchange-correlation potential close to as well as far from the metal surface. It therefore goes beyond the conventional Fowler-Nordheim treatment of field emission from a metal surface. We illustrate the utility of our method by calculating the field-emission current from a model jellium surface, using a local-density approximation exchange-correlation potential, modified to include the correct  $\sim 1/4x$  asymptotic behavior in the vacuum region. We find that the Fowler-Nordheim behavior can be recovered in the limit of low fields; in the limit of high fields, where the details of the self-consistent effective potential in the neighborhood of the surface become important, meaningful deviations from the Fowler-Nordheim current result.

### I. INTRODUCTION

The field-assisted emission of electrons from a metal surface is well described by the Fowler-Nordheim (FN) theory,<sup>1</sup> which is based on the free-electron theory of metals. Within this theory, the potential energy of an electron on the vacuum side of the metal-vacuum interface (measured relative to the bottom of the conduction band) is approximated by  $E_F + \phi - e^2/4x - eFx$ , where the four terms are the Fermi energy, the work function, the *classical* image potential, and the potential due to an external electric field, respectively;  $x$  is the distance perpendicular to the surface on the vacuum side,  $e$  is the electronic charge and  $F$  is the electric field. The FN theory leads to a very simple relationship between the emission current density and the applied electric field, in terms of just the work function of the metal surface.<sup>1</sup>

The above expression for the potential “seen” by an escaping electron is, however, valid only asymptotically (for  $x > 3 \text{ \AA}$  or so). The detailed shape of the barrier for  $x < 3 \text{ \AA}$  depends on the metal surface under consideration, and is not well represented in the FN treatment.<sup>2</sup> Calculation of the field-emission current using an accurate electronic structure method with proper treatment of the exchange-correlation interaction not only remedies this problem, but also incorporates system and surface specific band-structure effects (which are absent in the FN treatment). In the present study, we derive an expression for the field emission current using the Bardeen transfer Hamiltonian (BTH) method,<sup>3</sup> applicable to electronic structure treatments of the metal surface. The advantage of using the BTH formalism (as opposed to the calculation of the tunneling current using intensive scattering-theoretic techniques<sup>4</sup>) is that just the *stationary states* of the *isolated field-free* emitting system can be used to calculate the field-emission current.

As an illustrative example, we use the BTH method to calculate the field-emission current from a jellium surface. In the jellium model, the bulk solid is represented by a uniform

electron gas moving in a neutralizing uniform positive background, while at the surface, although the positive background is rigid, the electrons are allowed to relax and leak out into the vacuum in order to minimize their kinetic energy.<sup>5</sup> The jellium model provides us with a simple situation wherein the present method can be used to recover results already known in certain limiting cases (viz., the Fowler-Nordheim description in the low-field limit). The wave functions and potential of the jellium system are determined self-consistently<sup>5</sup> using a modified version of the local-density approximation<sup>6</sup> (LDA) within density-functional theory<sup>7</sup> (DFT). Although LDA has been widely and successfully used in treating many bulk and surface properties,<sup>6</sup> it has the incorrect asymptotic behavior of exponential decay (rather than the correct  $\sim 1/4x$  image behavior) outside of a surface in the vacuum region.<sup>8</sup> Hence, we use a modification suggested earlier by Serena *et al.*<sup>9</sup> in which the LDA potential inside the metal is interpolated smoothly (henceforth referred to as ILDA) to the classical image potential outside in the vacuum region. Thus, electron-electron correlations close to the surface are treated more realistically here than in the FN treatment, which, as we had mentioned earlier, accounts correctly only for the correlations far from the surface.

Although the ILDA is constructed in an *ad hoc* manner, we note that it is adequate for the illustration of the utility of the BTH method we are attempting here. Besides, the ILDA functional is easy to implement. For these reasons, we prefer the ILDA to other more sophisticated exchange-correlation functionals (e.g., the weighted-density approximation<sup>10</sup>) that naturally have the correct asymptotic behavior. It is worth mentioning that the present work is a first step towards a quantitative study of field emission from surfaces covered with adsorbates or coatings, or even nonplanar surfaces; we emphasize, though, that such quantitative studies require realistic treatment of surfaces, using atomistic electronic structure methods and exchange-correlation potentials more sophisticated than ILDA.

This paper is organized as follows. In the next section, we derive an expression for the field-emission current using the BTH formalism in terms of jellium wave functions, eigenvalues, and the self-consistent effective one-electron potential, and generalize it for use within atomistic plane-wave-based electronic structure methods. Our results for a model jellium system are presented and discussed in Sec. III, and we conclude with a brief summary. Details about the jellium calculations specific to the present implementation are given in the Appendix.

## II. BARDEEN TRANSFER HAMILTONIAN METHOD FOR CALCULATING THE FIELD-EMISSION CURRENT

Within the BTH formalism,<sup>3</sup> the left-hand side (cathode) and right-hand side (anode) systems are considered separately and the eigenfunctions and eigenvalues determined. The tunneling current from the left to right is then calculated using information about both the right- and left-hand side systems in the barrier region. We now derive an explicit expression for the tunneling or field-emission current assuming that the left-hand side system is modeled as a jellium slab. We then generalize our result for use in plane-wave-based atomistic electronic structure methods.

The wave functions and the energy eigenvalues of the left-hand side jellium system are determined in the absence of an electric field, as described in the Appendix. The extension of the wave functions into the barrier region in the presence of an electric field is obtained by using the WKB approximation. The right-hand side system in the case of field emission is composed of electrons that have tunneled through the barrier. The wave functions of this system in the barrier region are also determined using the WKB approximation. Assuming that the jellium surface normal (and the electron emission direction) are along the  $x$  axis, the left- and right-hand side wave functions,  $\Psi_{L,R}(x,y,z)$ , can be written as  $\psi_{l,r}(x)e^{i(k_y^{L,R}y+k_z^{L,R}z)}$  ( $L$  and  $R$  index the left- and right-hand side systems, i.e.,  $L \equiv \{l, k_y^L, k_z^L\}$  and  $R \equiv \{r, k_y^R, k_z^R\}$ ), where  $k_y^{L,R}$  and  $k_z^{L,R}$  are the wave vectors along the  $y$  and  $z$  directions. The left- and right-hand side eigenvalues  $E_{L,R}$  may be written as  $\epsilon_{l,r} + (k_y^{L,R})^2 + (k_z^{L,R})^2$ , where  $\epsilon_{l,r}$  are the ‘‘normal’’ energies. We then have the following expression for  $\psi_{l,r}(x)$  in the barrier region within the WKB approximation:<sup>11</sup>

$$\psi_{l,r}(x) = \frac{C_{l,r}}{2} |\kappa_{l,r}|^{-1/2} \exp\left(\alpha_{l,r} \int_{x_{l,r}}^x |\kappa_{l,r}| dx\right), \quad (1)$$

where  $\kappa_{l,r} = \sqrt{(2m/\hbar^2)[v_{eff}(x) - eFx - \epsilon_{l,r}]}$ ,  $m$  and  $e$  are the electron mass and charge, respectively,  $\hbar = h/(2\pi)$ , where  $h$  is Planck’s constant,  $v_{eff}(x)$  is the effective potential ‘‘seen’’ by an electron,  $F$  is the electric field,  $\alpha_l = -1$  and  $\alpha_r = +1$ , and  $x_{l,r}$  are the ( $\epsilon_{l,r}$ -dependent) turning points of  $v_{eff}(x)$ .  $C_{l,r}$  are normalization constants, which for the right-hand side system is expressed in terms of its density of states,<sup>11</sup>  $\theta_r(\epsilon_r)$ , i.e.,  $C_r = \sqrt{(2m/\hbar^2)/[\pi\theta_r(\epsilon_r)]}$ .  $C_l$  is determined by matching  $\psi_l(x)$  to the jellium wave function,  $\phi_l(x)$ , at a suitable point (say,  $x'_l$ ), typically about 1 a.u. to the right of the turning point  $x_l$ . This procedure is warranted by the fact that the WKB approximation breaks down at the immediate neighborhood of the turning point, and that  $x'_l$  can

be adjusted to ensure near continuity of the derivatives of  $\psi_l(x)$  and  $\phi_l(x)$ .  $C_l$  is thus given by

$$2\phi_l(x_l) |(2m/\hbar^2)[v_{eff}(x_l) - eFx_l - \epsilon_l]^{1/4} \exp\left(\int_{x_l}^{x'_l} |\kappa_l| dx\right).$$

The exponential term can be neglected if the distance  $x'_l - x_l$  is chosen to be much smaller than the exponential decay length.

The tunneling current is then given by<sup>3</sup>

$$I = \frac{4\pi e}{\hbar} \sum_{LR} |M_{LR}|^2 \delta(E_L - E_R), \quad (2)$$

with  $M_{LR}$  being the tunneling matrix element,

$$\begin{aligned} M_{LR} &= \frac{\hbar^2}{2m} \int_{x=\bar{x}} dy dz \left( \Psi_L^*(x,y,z) \frac{\partial}{\partial x} \Psi_R(x,y,z) \right. \\ &\quad \left. - \Psi_R(x,y,z) \frac{\partial}{\partial x} \Psi_L^*(x,y,z) \right) \\ &= \frac{\hbar^2}{2m} \left( \psi_l(x) \frac{\partial}{\partial x} \psi_r(x) \right. \\ &\quad \left. - \psi_r(x) \frac{\partial}{\partial x} \psi_l(x) \right) \Bigg|_{x=\bar{x}} \delta_{k_y^L, k_y^R} \delta_{k_z^L, k_z^R}. \end{aligned} \quad (3)$$

The integral in the first equation is performed along any plane  $x = \bar{x}$  entirely in the classically forbidden barrier region. Note that both  $\psi_l(x)$  and  $\psi_r(x)$  are required only in the barrier region.

Substituting  $M_{LR}$  into the expression for the total current yields

$$\begin{aligned} I &= \frac{4\pi e}{\hbar} \sum_l \sum_r \Bigg| \frac{\hbar^2}{2m} \left( \psi_l(x) \frac{\partial}{\partial x} \psi_r(x) \right. \\ &\quad \left. - \psi_r(x) \frac{\partial}{\partial x} \psi_l(x) \right) \Bigg|_{x=\bar{x}}^2 \delta(\epsilon_l - \epsilon_r) \\ &= \frac{4\pi e}{\hbar} \sum_l \sum_r \int d\epsilon_r \theta_r(\epsilon_r) \Bigg| \frac{\hbar^2}{2m} \left( \psi_l(x) \frac{\partial}{\partial x} \psi_r(x) \right. \\ &\quad \left. - \psi_r(x) \frac{\partial}{\partial x} \psi_l(x) \right) \Bigg|_{x=\bar{x}}^2 \delta(\epsilon_l - \epsilon_r). \end{aligned} \quad (4)$$

Noting that

$$\begin{aligned} \frac{\partial}{\partial x} \psi_{l,r}(x) &= \frac{C_{l,r}}{2} \exp\left(\alpha_{l,r} \int_{x_{l,r}}^x |\kappa_{l,r}| dx\right) \left[ \alpha_{l,r} |\kappa_{l,r}|^{1/2} \right. \\ &\quad \left. + \frac{2m}{\hbar^2} \left( \frac{eF}{4} - \frac{1}{4} \frac{dv_{eff}(x)}{dx} \right) |\kappa_{l,r}|^{-5/2} \right], \end{aligned} \quad (5)$$

the expression for the total current can be simplified to

$$I = \frac{4\pi e}{\hbar} \sum_l \sum_r \left( \frac{\hbar^2}{2m} \right) \frac{C_l^2}{4\pi} \exp\left(-2 \int_{x_l}^{x_r} |\kappa_l| dx\right). \quad (6)$$

Due to the cylindrical symmetry of the jellium problem, and since  $k_y^L$  and  $k_z^L$  form a continuum, the sum over  $k_y^L$  and  $k_z^L$  can be converted to an integration of the form

$$\begin{aligned} \sum_{k_y^L k_z^L} &\rightarrow \frac{\sigma}{(2\pi)^2} \int_0^{2\pi} d\phi \int_0^{\sqrt{k_F^2 - 2m\epsilon_l/\hbar^2}} k dk \\ &= \frac{\sigma}{4\pi} (E_F - \epsilon_l) (2m/\hbar^2), \end{aligned}$$

where  $\sigma$  is the cross-sectional area, and  $E_F$  is the Fermi energy. Finally, the field-emission current density,  $J$  ( $=I/\sigma$ ), is given by

$$J = \frac{e}{4\pi\hbar} \sum_l (E_F - \epsilon_l) C_l^2 \exp\left(-2 \int_{x_l}^{x_r} |\kappa_l| dx\right). \quad (7)$$

The present method can be incorporated in traditional plane-wave-based atomistic electronic structure schemes to calculate field-emission currents from surfaces. In such cases, the left-hand side system wave functions are written in a Laue representation:  $\Psi_L(\mathbf{r}) = e^{i\mathbf{k}_\parallel \cdot \mathbf{r}_\parallel} \sum_{\mathbf{G}_\parallel} e^{i\mathbf{G}_\parallel \cdot \mathbf{r}_\parallel} \phi_{l\mathbf{k}_\parallel \mathbf{G}_\parallel}(x)$ , where now  $L \equiv \{l, \mathbf{k}_\parallel\}$ , with  $\mathbf{k}_\parallel$  being a  $\mathbf{k}$  point in the first surface Brillouin zone,  $\mathbf{r}_\parallel$  represents a vector in the  $yz$  plane, and  $\mathbf{G}_\parallel$  is a two-dimensional (2D) reciprocal-lattice vector in the  $yz$  plane. This form of  $\Psi_L(\mathbf{r})$  when used in the BTH formalism results in the total current

$$I = \frac{4\pi e}{\hbar} \sum_l \sum_{\mathbf{k}_\parallel} \left( \frac{\hbar^2}{2m} \right) \frac{C_{l\mathbf{k}_\parallel 0}^2}{4\pi} \exp\left(-2 \int_{x_l}^{x_r} |\kappa_{l\mathbf{k}_\parallel 0}| dx\right), \quad (8)$$

where now,

$$C_{l\mathbf{k}_\parallel 0} = 2 \phi_{l\mathbf{k}_\parallel 0}(x_l) | (2m/\hbar^2) [v_0(x_l) - Fx_l - \epsilon_{l\mathbf{k}_\parallel}] |^{1/4}$$

with  $\epsilon_{l\mathbf{k}_\parallel} = E_L - \hbar^2 k_\parallel^2 / 2m$ ,

$$\kappa_{l\mathbf{k}_\parallel 0} = \sqrt{(2m/\hbar^2) [v_0(x) - eFx - \epsilon_{l\mathbf{k}_\parallel}]},$$

and  $v_0(x)$  is the  $\mathbf{G}_\parallel = \mathbf{0}$  component of the 2D Fourier transform of the effective potential. In this expression, we have assumed that the corrugation of the potential and the wave functions along the  $yz$  plane can be neglected on the scale of the barrier width (the former is of the order of angstroms, and the latter, for fields in typical field-emission experiments, is of the order of tens of angstroms). It is worth mentioning that the local band-structure effects (or the local density of states information) are introduced in the current through the energy spectrum, and the summation over  $l$ ; thus, effects due to adsorbates on surfaces—such as resonant tunneling—will be captured within this treatment, provided  $x_l$  is chosen to be to the right of the adsorbate (not just to the right of the metal surface). Although in the clean metal or jellium cases, we could assume that the electric field does not perturb the left-hand side system wave functions and eigenvalues, this may not be a valid assumption for adsorbate-covered metal surfaces (due to field penetration through the adsorbate). In such cases, the perturbed left-hand side wave functions (at  $x_l$ ) and eigenvalues can be obtained from their unperturbed counterparts using first-order perturbation theory with the electric field treated as a perturbation. The

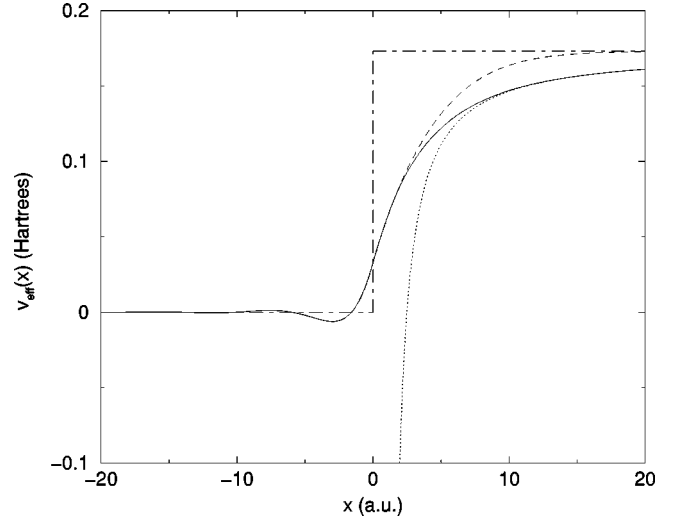


FIG. 1. Total self-consistent LDA (dashed line) and ILDA (solid line) effective potentials relative to their bulk values as a function of distance from the surface;  $x > 0$  and  $x < 0$  represent vacuum and jellium, respectively. The classical image potential and the step potential at the surface are represented by dotted and dot-dashed lines, respectively.

present work thus paves the way for a quantitative study of the field-emission current from adsorbates, coatings, and oxides, and is a first step towards a study of nonplanar surfaces (such as Spindt tips and nanoprotusions).

As an aside, we point out that the FN expression<sup>1</sup> for the current density can be recovered from the jellium BTH expression [Eq. (7)] derived above. Within the free-electron gas model, which underlies the FN treatment,  $C_l = \sqrt{(2m/\hbar^2)/[\pi\theta_l(\epsilon_l)]}$ . After converting the sum over the left-hand side system to an integration  $[\sum_l \{ \dots \} \rightarrow \int_0^{E_F} d\epsilon_l \theta_l(\epsilon_l) \{ \dots \}]$ , and replacing the jellium effective potential by the one used in the FN treatment,

$$J^{FN} = \frac{em}{2\pi^2\hbar^3} \int_0^{E_F} (E_F - \epsilon) \exp\left(-2 \int_{x_l}^{x_r} |\kappa^{FN}| dx\right) d\epsilon, \quad (9)$$

where  $\kappa^{FN} = \sqrt{(2m/\hbar^2)(E_F + \phi - e^2/4x - eFx - \epsilon)}$ . It can be shown that the above expression for  $J^{FN}$  results precisely in the FN expression when the appropriate approximations are made.<sup>1</sup>

### III. RESULTS AND DISCUSSION

We consider as a model system a jellium surface with an average density corresponding to  $r_s = 5.0$  ( $r_s$  is defined as the average radius of an electron, as  $4\pi r_s^3 \bar{\rho}/3 = 1$ , where  $\bar{\rho}$  is the average valence electron density of the bulk metal); for comparison, we mention that K, Rb, and Cs have  $r_s$  values of 4.96, 5.23, and 5.63, respectively.<sup>8</sup> In Fig. 1, we show the self-consistent LDA and ILDA effective potentials in the neighborhood of the surface of the slab, whose long-range behavior is dominated by the exchange-correlation potential. For comparison, we also show the step potential at the surface, and the classical image potential whose form is given by  $1/4(x - x_{image})$ .  $x_{image}$  was calculated earlier<sup>9</sup> self-consistently as the centroid of a small amount of excess

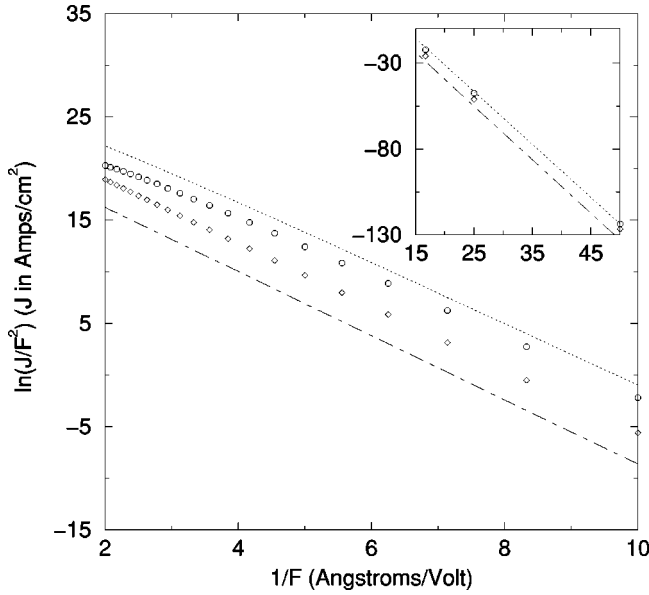


FIG. 2. Fowler-Nordheim plot of the current densities calculated using the jellium model with LDA (diamonds) and ILDA (circles) exchange-correlation potentials. Dot-dashed and dotted lines represent results obtained using the Fowler-Nordheim equation without and with image potential, respectively. Inset shows the same plot for low fields.

charge added to the system; for a system with  $r_s = 5.0$ ,  $x_{image}$  was found to be 1.08 a.u.<sup>12</sup> The LDA potential has a rapid decay following the exponential decay of the electronic density. The ILDA potential, on the other hand, has the correct asymptotic behavior, and recovers the LDA result inside the jellium. Clearly, the classical image potential assumed in the FN treatment is quite inadequate in regions close to the surface. In the vacuum region, both the self-consistent LDA and ILDA effective potentials are bounded by the classical image potential and the step potential. It can thus be anticipated that both the LDA and ILDA tunneling currents will be somewhere between the FN currents calculated with and without the image potential. Furthermore, it can also be expected that the current calculated using the ILDA potential will be between that calculated using the LDA potential and FN current calculated using the image potential.

The actual calculation of the tunneling current density using the BTH formalism confirm these expectations. Figure 2 shows the calculated current density as a function of field in a typical Fowler-Nordheim plot. For comparison, we also show the FN results with and without the image potential; these curves were generated using the FN equation<sup>1</sup> for the calculated jellium work function of 2.74 eV [the work function is defined as  $v_{eff}(\infty) - E_F$ ].<sup>13</sup> Two interesting points are worth mentioning: (i) in the limit of low fields (shown as the inset in Fig. 2), the ILDA current approaches the FN result with image potential; this is clearly understandable since at low fields, the barrier width is so large that details of the effective potential close to the surface become irrelevant (at these low fields, the LDA current density is lower than the ILDA current density because the LDA barrier approaches the vacuum level more rapidly), (ii) in the limit of high fields, significant deviations of the ILDA current towards the LDA result and away from the FN current can be seen; this is again reasonable since at high fields, the asymptotic behavior

of the effective potential becomes relatively unimportant compared to its behavior close to the surface (where the FN treatment breaks down, and the LDA and ILDA potentials coalesce).

#### IV. SUMMARY

A crucial outcome of this work is the development of a method, using the Bardeen transfer Hamiltonian formalism, to calculate the field-emission current from planar surfaces. This method can be directly incorporated in large-scale atomistic electronic structure methods, as it requires only the knowledge of the field-free self-consistent potential in the vacuum region, the energy spectrum and the value of the wave functions at the turning point of the potential outside the surface, all of which are available from standard electronic structure calculational schemes. Using a realistic exchange-correlation potential (e.g., the weighted-density approximation) that possesses the correct asymptotic behavior in such electronic calculations will yield results more quantitative than those obtained using the Fowler-Nordheim formula (which cannot describe local electronic structure and adsorbate-induced resonant effects). The present work is the first step towards a quantitative study of the field-emission current from nonplanar structures such as Spindt tips and nanoprotusions.

We have used a model jellium surface as a test system in this study. Our results for this test system can be summarized as follows: the calculated tunneling current for the jellium system is bounded by the FN results obtained assuming just the step potential at the surface, and a classical image potential in addition to the step potential. In the limit of low fields the jellium current approaches the FN (with image potential) current as details of the form of the actual potential close to the surface become unimportant due to the largeness of the barrier. In the limit of high fields, the jellium current deviates (decreases) from the FN value, as in this limit the barrier width is small, and the form of the effective potential close to the surface becomes important.

#### APPENDIX: JELLIUM CALCULATION

Our model jellium system is constructed slightly differently compared to the original Lang-Kohn (LK) treatment.<sup>5</sup> While in their case they had a semi-infinite slab extending from  $x=0$  to  $x=-\infty$ , we have a slab of thickness  $d$  centered at the origin. Thus, our jellium slab is symmetric about  $x=0$ , and the positive background for our system,  $\rho_+(x)$ , is given by

$$\rho_+(x) = \begin{cases} \bar{\rho}, & |x| \leq d/2 \\ 0, & |x| > d/2, \end{cases} \quad (\text{A1})$$

where  $\bar{\rho}$  is the average electron density (number of valence electrons per Wigner-Seitz cell/volume of a Wigner-Seitz cell) of the system.

For this model system, the wave functions and energies are given by<sup>5</sup>

$$\Psi_{k,k_y,k_z}(x,y,z) = \phi_k(x) e^{i(k_y y + k_z z)}, \quad (\text{A2})$$

$$E_{k_x, k_y, k_z}(x, y, z) = \epsilon_k + \hbar^2(k_y^2 + k_z^2)/2m. \quad (\text{A3})$$

Since our model system is a slab finite in the  $x$  direction, the energies  $\epsilon_k$  do not form a continuum, unlike in the LK treatment.  $\epsilon_k$  and the associated  $\phi_k(x)$  are determined by self-consistently solving the following set of Hohenberg-Kohn-Sham equations (in Hartree atomic units):

$$\left( -\frac{1}{2} \frac{\partial^2}{\partial x^2} + v_{eff}(\rho(x)) \right) \phi_k(x) = \epsilon_k \phi_k(x), \quad (\text{A4})$$

$$v_{eff}(\rho(x)) = -4\pi \int_x^\infty dx' \int_{x'}^\infty dx'' [\rho(x'') - \rho_+(x'')] + \mu_{xc}(\rho(x)) + \Delta\Phi, \quad (\text{A5})$$

$$\rho(x) = \frac{1}{\pi} \sum_{k \leq k_F} (E_F - \epsilon_k) |\phi_k(x)|^2, \quad (\text{A6})$$

where  $\rho(x)$  is the electronic density and  $v_{eff}(\rho(x))$  is the effective potential. The effective potential is composed of the electrostatic (first term) and exchange-correlation (second term) contributions. The last term in  $v_{eff}(\rho(x))$ ,

$$\Delta\Phi = 4\pi \int_0^\infty dx' \int_{x'}^\infty dx'' [\rho(x'') - \rho_+(x'')] - \mu_{xc}(\bar{\rho}), \quad (\text{A7})$$

is included so that  $v_{eff}(\rho(x))$  is zero at  $x=0$ ; this way, all allowed energies in the bulk region are positive.  $E_F$  is the bulk Fermi energy given in terms of the average charge den-

sity by  $E_F = k_F^2/2 = (3\pi^2\bar{\rho})^{1/3}/2$ , and  $k_F$  is the bulk Fermi wave vector.

In treating the exchange-correlation interaction between electrons, we have used both the widely used local-density approximation (LDA) with the Wigner form for the correlation potential,<sup>5</sup> and a functional form proposed by Serena *et al.* (ILDA).<sup>9</sup> LDA does not have the correct asymptotic behavior in the vacuum region, where it has an exponential decay rather than the correct  $\sim 1/4x$  behavior. The ILDA form corrects this error self-consistently; it recovers the LDA result in the bulk region, and smoothly interpolates it outside the image plane to the classical  $1/4(x - x_{image})$  image potential,  $x_{image}$  being the location of the image plane which, in general, does not coincide with the physical surface of the metal.<sup>8</sup> It should thus be noted that ILDA does *not* improve the LDA in the bulk and surface regions, but just complements it by including the image potential more realistically in the vacuum region.

The set of Hohenberg-Kohn-Sham equations are solved in the following manner. A trial charge density distribution, as proposed by Perdew *et al.*,<sup>14</sup> is chosen. The kinetic energy term in the Hamiltonian is discretized using a three-point finite difference formula, periodic boundary conditions are imposed, and the period  $L$  of the system is taken sufficiently large compared to the slab thickness  $d$ , so that the effective potential has enough room to flatten out. The resulting Hamiltonian matrix is tridiagonal in real space and can be diagonalized efficiently.<sup>15</sup> A direct inversion of iterative subspace (DIIS) procedure<sup>16</sup> was used to mix the new charge density with the earlier ones providing a stable and fast convergence to the self-consistent result. A slab of thickness 420 a.u. was used in this study.

<sup>1</sup>R.H. Fowler and L.W. Nordheim, Proc. R. Soc. London, Ser. A **119**, 173 (1928); L.W. Nordheim, *ibid.* **121**, 626 (1928); A. Modinos, *Field, Thermionic, and Secondary Electron Emission Spectroscopy* (Plenum Press, New York, 1984).

<sup>2</sup>The literature on defects of the Fowler-Nordheim treatment, and remedies, is vast; we refer the interested reader to the following related articles: M.G. Ancona, Phys. Rev. B **46**, 4874 (1992); P.H. Cutler, Jun He, N.M. Miskovsky, B. Weiss, and T.E. Sullivan, Prog. Surf. Sci. **42**, 169 (1993); Peter Lerner, P.H. Cutler, and N.M. Miskovsky, J. Vac. Sci. Technol. B **15**, 337 (1997), K.L. Jensen, J. Appl. Phys. **85**, 2667 (1999), and references therein.

<sup>3</sup>J. Bardeen, Phys. Rev. Lett. **6**, 57 (1961).

<sup>4</sup>A.A. Lucas, H. Morawitz, G.R. Henry, J.-P. Vigneron, Ph. Lambin, P.H. Cutler, and T.E. Feuchtwang, Phys. Rev. B **37**, 10708 (1988); Kenji Hirose and Masaru Tsukada, *ibid.* **51**, 5278 (1995).

<sup>5</sup>N.D. Lang and W. Kohn, Phys. Rev. B **1**, 4555 (1970).

<sup>6</sup>A. R. Williams and U. von Barth, in *Theory of the Inhomogeneous Electron Gas*, edited by S. Lundquist and N. H. March (Plenum, New York, 1983).

<sup>7</sup>P. Hohenberg and W. Kohn, Phys. Rev. B **136**, 864 (1964); W. Kohn, and L.J. Sham, Phys. Rev. A **140**, 1133 (1965).

<sup>8</sup>A. Kiejna and K. F. Wojciechowski, in *Metal Surface Electron Physics* (Elsevier, New York, 1996), pg. 153, and references therein.

<sup>9</sup>P.A. Serena, J.M. Soler, and N. Garcia, Phys. Rev. B **34**, 6767 (1986).

<sup>10</sup>O. Gunnarsson, M. Jonson, and B.I. Lundqvist, Phys. Rev. B **20**, 3136 (1979); O. Gunnarsson and R.O. Jones, Phys. Scr. **21**, 394 (1980).

<sup>11</sup>W.A. Harrison, Phys. Rev. **123**, 85 (1961).

<sup>12</sup>The location of the image plane may change with respect to the applied electric field. Thus, a more realistic treatment of the surface requires not just explicitly treating the atoms, but also using more sophisticated exchange-correlation potentials instead of the ILDA.

<sup>13</sup>N.D. Lang and W. Kohn, Phys. Rev. B **3**, 1215 (1971).

<sup>14</sup>J.P. Perdew, H.Q. Tran, and E.D. Smith, Phys. Rev. B **42**, 11 627 (1990).

<sup>15</sup>See, for example, routines available at [www.netlib.org](http://www.netlib.org).

<sup>16</sup>P. Pulay, Chem. Phys. Lett. **73**, 393 (1980).